Integrated Drive Train and Structural Optimization for a Dynamic System: An Evolving Conceptual Design Algorithm

Musa Ozgun Gulec, Seniz Ertugrul

Abstract— **Selecting the most suitable motor sizes, gear boxes and structure under certain constraints or desired values such as payload, speed, deflections, total weight, etc. for a dynamic system is an exhaustive and time-consuming iterative process. To overcome this problem, a new-"evolving" conceptual design algorithm is developed. The suggested algorithm can be used for the conceptual design of any dynamic system including drive-train and structural optimization. To illustrate the suggested methodology, a robot manipulator, having 3 degrees of freedom, is selected as a case study. The objective function is minimizing the robot mass while satisfying the desired dynamic requirements and constraints of link deflections. A dynamic simulation environment for flexible body motion, containing 3 DOF robot manipulator drive-trains and flexible links, is developed in an evolving optimization loop. The lumped parameter estimation method is used to model the flexibility of uniform links in Simmechanics by allowing the estimation of deflections caused by the dynamic motion. Thus, both dynamic and structural simulations are made simultaneously in Simmechanics with no additional software. Hence, drive-trains and thickness of all links are simultaneously optimized by using the suggested evolving conceptual design algorithm.**

Key Words: Robot design, integrated conceptual design optimization, dynamic simulation of flexible bodies, the lumped parameter estimation, drive-train optimization.

I. INTRODUCTION

Designing a multi body dynamic system is a very complex, time consuming and iterative process. These difficulties generate a necessity of conceptual design process to select roughly the drive-train and sizes of structures. This study not only creates a conceptual design of a dynamic system but also generalizes the conceptual design process for a specific dynamic system via extensive drive-train library and fully variable dependent algorithm. Hence an evolving conceptual design algorithm, that can constitute an optimum conceptual design of a dynamic system by considering the design parameters and constraints, is created. 3 DOF robot manipulator is selected as a case study to illustrate the evolving conceptual design algorithm. Besides, increasing demand for improving robot manipulator efficiency makes robot manipulator design optimization a crucial subject. There are several studies about the robot manipulator efficiency and design optimization from different points of view. One of them is a kinematic optimization that was applied to an existing manipulator and selected the optimum link lengths [1]. Then, there is a drive-train optimization study in literature. Drive-trains were selected among specific motors and gearboxes via dynamic simulation [2]. An integrated drive-trains and dimensional optimization also exists in literature. In that study, the rate of link lengths was optimized to obtain better kinematic performance and the drive-trains optimization made the dynamic capability better. The dynamic simulation was also used and once again, the drive trains were selected among a specific list of motors and gearboxes [3]. There is another study about overall manipulator design optimization including kinematics, dynamics, drive-trains, and structure. Again, the aim was to optimize the rate of link lengths to increase kinematic performance, and the drive-trains optimization provided better dynamic capability. Additionally, strength optimization achieved the optimum structure [4][5][6]. These five studies, mentioned above, belong to the same researchers. All the studies used MATLAB to create an optimization loop, made dynamic simulation in ADAMS, and simulated static strength analysis in ANSYS. Therefore, they used 3 different software simultaneously. The strength analysis could only be done while the manipulator is static in a certain position. Besides, the optimization focused on the final design of a specific robot manipulator instead of a conceptual design of a non-specific manipulator. Then, there were very few motors and gearbox alternatives to be used in the optimization loop. There are also some other studies about design optimization such as sequential optimization of kinematic and dynamic performance [7], drive-train optimization [8][9], integrated topology and parametric system optimization [10], topology optimization of a robot arm [11], kinematic optimization [12][13], dynamic optimization of flexible robot arm [14][15][16].

This study illustrates an integrated drive-train and structural optimization of a robot manipulator conceptual design due to their direct impacts on each other. In serial robot manipulators, the masses of the drive-trains directly affect both dynamic behavior and link deflections. Indeed, while designing a manipulator, more powerful and durable yet heavier drive-train can improve dynamic behavior but causes more deflections in the links and increases the tip point error. Even, in some cases, more powerful drive-train both degrades dynamic capability and increases tip point deflection because of increment of its mass. Therefore, drive-trains and structure of the links must be simultaneously designed and optimized for a robot manipulator. Unlike literature, this study focuses on obtaining the optimum

F. Musa Ozgun Gulec is with the Istanbul Technical University, Istanbul - Turkey (corresponding author to provide phone: 0090-507-705-8644; e-mail: ozgun_gulec@yahoo.com).

S. Seniz Ertugrul is with Izmir University of Economics, Izmir - Turkey, (e-mail: seniz.ertugrul@izmirekonomi.edu.tr).

conceptual design of a robot arm, not a final design. It means that, this algorithm can find optimum conceptual design for any size of robot manipulators. The sizes of the robot links can be determined by user in the beginning of the algorithm and there is a wide variety library containing 31 different DC motors and 675 different gearboxes. Besides, this methodology uses only MATLAB and it does not need any additional software like ANSYS or ADAMS. This makes the methodology more comfortable, easy to use, and less time-consuming. The final and the most important contribution is the structural analysis. Both the structural and dynamic simulation can be done simultaneously in Simulink with the help of the lumped parameter estimation method. Therefore, the structure can be simulated under the dynamic forces during the motion unlike static structural analysis in ANSYS as in the literature. The aim is to create an optimum conceptual design of a 3 DOF robot manipulator, as seen in Figure 1, whose kinematic chain and workspace have been previously optimized or specified. The methodology is called evolving conceptual design algorithm and the algorithm both obeys the design parameters and constraints then, searches the optimum conceptual robot design via dynamic simulation in the Simmechanics environment. After achieving optimum conceptual design, topology optimization can be applied sequentially to increase efficiency and create a detailed design.
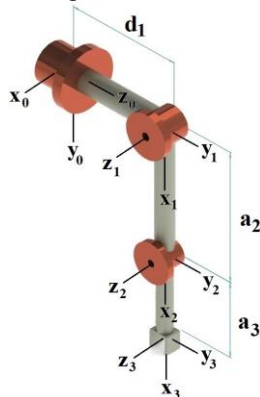

Figure 1.   3 DOF robot manipulator.

II.   DRIVE TRAIN LIBRARY

The drive-train library, consisting of 35 DC motors and 675 Harmonic Drive gearboxes, is created. In the library, there are 20 different parameters for each DC motor and gearbox as given in the Table 1 and 2. Hence, a matrix of 20 x 35 constitutes the DC motor library while a matrix of 20 x 675 constitutes the Harmonic Drive gearbox library. The nonlinear torque-rpm graphics of motors are also created by using curve fitting method after obtaining sample points from the catalogue.

TABLE 1. MAXON DC MOTOR TECHNICAL DATA.

Motor Number	Speed / Torque (V/mNm)
Nominal Voltage (V)	Stall Torque (mNm)
Nominal Torque (mNm)	Time Constant (ms)
Nominal Current (A)	Rotor inertia (gcm^2)
Efficiency (%)	Max. Speed (rpm)
Power (W)	Max. axial load (N)
No Load Speed (rpm)	Max. radial load (N)
No Load Current (mA)	Weight (g)
Toque Constant (mNm/A)	Length (mm)
Speed Constant (rpm/V)	Curve fit polynomial degree

TABLE 2 HARMONIC DRIVE TECHNICAL DATA.

Harmonic Drive Number
Size
Ratio
Repeated peak torque limit - T_R (Nm)
Average torque limit - T_A (Nm)
Rated torque at 2000 rpm - T_N (Nm)
Momentary peak torque limit - T_M (Nm)
Max. input speed (oil) - (rpm)
Max. input speed (grease) - (rpm)
Avg. input speed limit (oil) – (rpm)
Avg. input speed limit (grease)- (rpm)
Moment of inertia (gcm^2)
Weight (g)
Accuracy $(arcmin)$
Torsional stiffness torque 1- T1 (mNm)
Torsional stiffness torque 2- T2 (mNm)
Torsional stiffness 1 – K1 (mNm/rad)
Torsional stiffness 2 – K2 (mNm/rad)
Torsional stiffness 3 – K3 (mNm/rad)
Harmonic Drive General Sizes

The motors have a cylindrical shape and one single diameter and length. However, gearboxes have many sizes as seen in Figure 2. The library is used during optimization process.
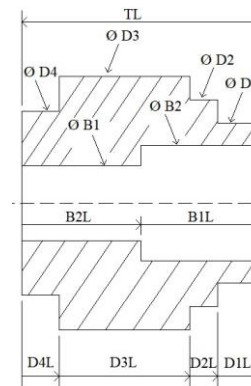

Figure 2.   Harmonic Drive general sizes.

III.   3 DOF ROBOT MANIPULATOR DESIGN VIA EVOLVING CONCEPTUAL DESIGN ALGORITHM

The evolving conceptual design algorithm consists of 5 loops inside as seen in Figure 3. Then, there are two different trajectories and two different dynamic simulation environments. One of the trajectories is based on a cubic velocity profile and is used nominally. The other one has a trapezoidal velocity profile and is used for a sudden stop in emergencies. The first dynamic simulation environment is based on rigid body dynamics and is used to observe the dynamic behavior of the robot. The second one is called flexible dynamic simulation that is used in structural optimization, and it can show the deflections in the bodies. Flexible structure is created by using the lumped parameter estimation method. Before optimization loop, the design parameters and constraints should be determined. There are 5 design parameters which are desired robot workspace (d_1, a_2, a_3), time to maximum speed (tm_{max}), structure material (steel or aluminum), initial thicknesses of links (t_i) and, increment of thickness (t_{inc}). Then, there are 7 constraints which are joints maximum cycle time $(t_{max.cycle})$, safety factor for motor , maximum payload (m_{max}), sudden stop maximum deceleration (af_{sudden}), maximum Harmonic Drive permissible twist $(\theta_{HD}$ 'arc-min'), maximum permissible tip point error

during motion ($err_{dynamic}$) and, maximum permissible static tip point error (err_{static}). The optimization cycle is explained step by step below.
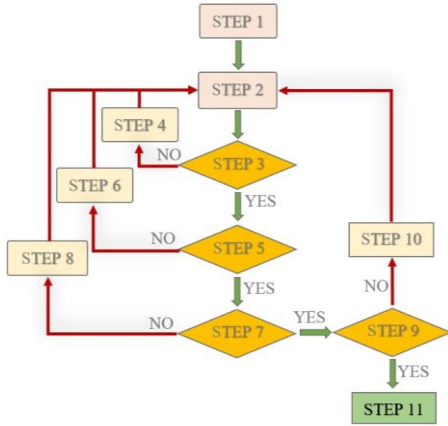

Figure 3.   Flowchart of Evolving Conceptual Design Algorithm.

Step 1: The design parameters and constraints are determined. Then, the required maximum angular velocities of links are obtained according to the design parameters and constraints. After that, the cubic and trapezoidal velocity profiles for nominal and sudden stop simulations are created. Finally, the optimization cycle starts with minimum weight DC motors.

Step 2: Harmonic Drive gearboxes that cannot comply with the desired velocities are eliminated from the library. Then, gearboxes, which are very big or small compared to the selected motors, are again eliminated roughly. This is just a rough elimination that provides less optimization time. To illustrate, if the motor's stall torque (maximum torque capability) is smaller than the gearbox's TN torque limit (minimum torque limit in the catalogue), it means that the motor is too small compared to the gearbox, and vice versa. After all eliminations, the rest are listed by weight and the cycle continues with the minimum weight.

Step 3: In this step, the minimum thicknesses of links are selected. The inner diameters are determined according to the average diameters of gearboxes. Then the variable dependent Simmechanics environment is created in pursuant of the whole data of motors, gearboxes, and the structure. Finally, the first dynamic simulation based on rigid body dynamics is performed. After simulation, motor's nonlinear torque-rpm (τ_M vs n) curves are created via curve fitting method. These curves are then compared with the simulation results (τ_{SD} vs n) by considering the M_{sf} (motor's safety factor). If the whole motors have sufficient capacity, cycle continues with step 5. If not, cycle continues with step 4 and returns to the beginning of the cycle.

Step 4: The insufficient motor or motors are changed with the next one and cycle is started again.

Step 5: This step checks whether gearboxes are sufficient for nominal operation. The torque limit values of harmonic drive gearboxes "T_R, T_A and T_N" are compared to the simulation results. Since the harmonic drives can resist momentarily higher than these limits, additional safety factor is not used. Then the angular deflections of gearboxes are calculated by using the torques of simulation results along with harmonic drive gearboxes' s torsional stiffness torques and torsional stiffness

values "$T1$, $T2$, $K1$, $K2$, $K3$". After that, they are compared to constraint of permissible twist angle limits (θ_{HD} 'arc-min') of gearboxes. Then, it is determined that the gearboxes are sufficient or not. Finally, if all of them are sufficient, cycle continues with Step 7. If at least one of the gearboxes is not sufficient, cycle continues with the Step 6 and returns to the beginning of the cycle.

Step 6: The insufficient gearbox or gearboxes are changed with the next one and the algorithm goes to the beginning of the cycle.

Step 7: In this step, the structure of the arm is evaluated. To observe deflections of links during the motion, the flexible dynamic simulation environment is created by using the lumped parameter method. In this method, each link is divided equally into sub-links in a finite number. In this study, each link is divided into 5 equal sub-links as shown in Figure 4. Then, each sub-link is connected via spherical joints. Finally, the spring coefficients of sub-links are calculated via Equation 1 and defined into the spherical joints.
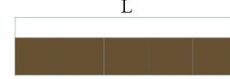

Figure 4.   Meshed link.

$$k_{sub-link} = \frac{3EI}{\left(\frac{L}{5}\right)} \left(\frac{Nm}{rad}\right) \qquad (1)$$

After running the flexible dynamic simulation in Simulink, the actual tip points during the motion can be obtained. Then, the differences between actual (flexible) and desired (nonflexible) tip points during the motion are calculated. Finally, the maximum difference gives the maximum dynamic error during the motion. That error is compared to the related constraint ($err_{dynamic}$). If the error is greater than the constraint, it must be determined which link has the maximum effect on tip point error. To find this, tip points of each link are sensed relative to their own bases in flexible dynamic simulation via body sensor property in Simmechanics. Figure 5 shows the deflections of links and angular errors "θ_{err1} , θ_{err2} , θ_{err3}" can be calculated by using equation 2 and 3.
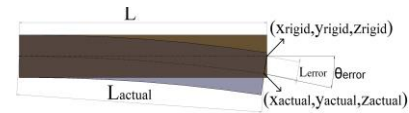

Figure 5.   Deflections of links.

$$L_{error} = \sqrt{\begin{array}{c}\left(z_{actual} - z_{rigid}\right)^2 + \\ \left(y_{actual} - y_{rigid}\right)^2 + \left(x_{actual} - x_{rigid}\right)^2\end{array}} \qquad (2)$$

$$\theta_{error} = \text{acos}\left(\frac{\left(L_{error}^2 - L^2 - L_{actual}^2\right)}{\left(-2 * L * L_{actual}\right)}\right) \qquad (3)$$

An extra virtual motor is added into the first link to observe the deflection effect of first link on tip point error. Then, the virtual DH parameters are obtained with respect to the new virtual 4 DOF robot manipulator as seen in Figure 6.

Firstly, the first link is accepted as flexible, and the others are accepted as rigid ($\theta_{err2} = 0$, $\theta_{err3} = 0$). Therefore, the first link becomes a single flexible part of the manipulator. Finally,

the tip point error that occurs because of the only first link is calculated via virtual DH parameters.

The same calculation is repeated for the other two links and their effects on tip point error are obtained. Then, it can now be determined which link is the most effective on the tip point error. Finally, that link is selected to increase its thickness. The next step is determining the total tip point deflection while the manipulator is static in a horizontal position as seen in Figure 7
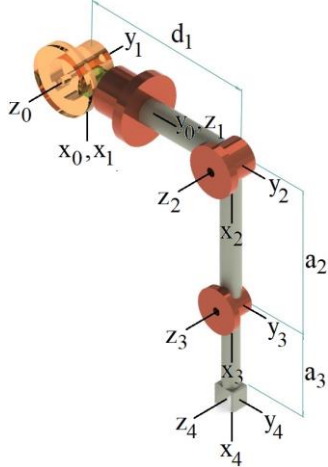

Figure 6.   Virtual 4 DOF robot manipulator configuration.

A horizontal position is selected while computing static deflection because this position is the worst case for static deflection. Then, this static tip point error is compared to the related constraint (err_{static}). If the error is greater than the constraint, related link which has maximum effect on tip point error is calculated as in dynamic tip point error e_{dtp} calculation.
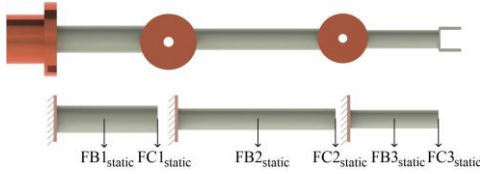

Figure 7.   3 DOF robot manipulator horizontal position.

As shown in the below side of Figure 7, the links are separated from each other, and all static forces are marked. They are accepted as a beam attached to a wall. The forces "$FB_{1static}, FB_{2static}$ and $FB_{3static}$" imply the weights of the links. The forces "$FC_{1static}, FC_{2static}$ and $FC_{3static}$" are the internal forces that contain payload and weights of motors, gearboxes, links. Then the static deflections "$ds_{1,2,3}$" of the links are calculated by using Equation 4. Static angular errors "$\theta s\_err_{1,2,3}$" that occur because of deflections are calculated with equation 5.

$$ds_{1,2,3} = -\frac{FC_{1,2,3} * L_{1,2,3}^{3}}{3 * E_{1,2,3} * I_{1,2,3}} - \frac{5 * FB_{1,2,3} * L_{1,2,3}^{3}}{24 * E_{1,2,3} * I_{1,2,3}} \quad (4)$$

$$\theta s\_err_{1,2,3} = \frac{ds_{1,2,3}}{d_{1,2,3}} \quad (5)$$

The next step is determining the static tip point error (e_{stp}). To obtain this, the actual (flexible body) tip point is calculated via forward kinematic equation including static angular errors

"$\theta s\_err_{1,2,3}$". The difference between actual and desired tip point gives the tip point static error. The desired tip point is also the horizontal position "$[0; 0; (d1 + a2 + a3)]$". Finally, the tip point static error is compared to related constraint which is the maximum permissible static tip point error (err_{static}). If the error is greater than the constraint, it must be determined which link has the maximum effect on the tip point error. The same procedure in dynamic tip point error case is repeated. Firstly, the first link is accepted as flexible, and the others are accepted as rigid. ($\theta s_{\_err2} = 0$, $\theta s_{\_err3} = 0$). The tip point error that occurs because of only first link is calculated via forward kinematic. The same calculation is repeated for other two links and their effects on tip point static error are obtained. Then, it can now be determined which link is the most effective on the tip point error. Finally, that link is selected to increase its thickness. If both dynamic and static tip point errors are lower than the related constraints, the cycle continues with Step 9. If not, cycle continues with Step 8 to increase thicknesses of insufficient structures.

Step 8: This step is to increase the thickness of the related link or links. If the selected to be increased links are same in both dynamic and static situation, only the related link's thickness is increased with amount of "Increment of thickness (t_{inc})". If they are different, the related two link's thicknesses are increased with amount of "Increment of the thickness (t_{inc})". After increment, the cycle continues with Step 2 and returns to the beginning of the cycle.

Step 9: This step checks whether gearboxes can endure in sudden stop situation. The first dynamic simulation environment which is based on rigid body motion is used. Besides, the second velocity profile which is trapezoidal is selected. The deceleration is increased to sudden stop maximum deceleration (af_{sudden}). After the dynamic simulation, the necessary torques for each link are obtained and the maximum necessary torques (τ_{peak}) are selected. These torque values are compared to gearboxes momentary peak torque limits - T_M (Nm). If at least one of the maximum torque exceeds the momentary peak torque limit T_M (Nm), the cycle continues with Step 10 and returns to the beginning of the cycle. If all maximum torques are lower than momentary peak torque, the cycle continues with Step 11.

Step 10: The insufficient gearbox or gearboxes are changed with the next one and the algorithm goes to the beginning of the cycle.

Step 11: This step means that the optimization for the desired task is concluded. The objective function of this optimization problem is obtaining the minimum weight robot design while satisfying the design parameters and constraints. Besides, there is no predetermined iteration number. The optimization cycle continues until finding the desired solution. Since there is a one objective function, the optimum solution is also unique.

IV. EXAMPLE CONCEPTUAL DESIGN RESULTS

To demonstrate the evolving conceptual design algorithm and results, there is an example whose design parameters and constraints are shown in Table 3 and Table 4 respectively. The trajectories for nominal and sudden stop situations are shown in Figure 8 and Figure 9 respectively.

TABLE 3 DESIGN PARAMETERS OF EXAMPLE OPTIMIZATION.

Desired robot workspace (d_1, a_2, a_3)	$(110,100,150)\ mm$
Time to maximum speed (tm_{max}).	$0,5\ s$
Structure material (steel or aluminum)	Steel
The initial thickness of links (t_i)	$3\ mm$
Increment of thickness (t_{inc})	$0,5\ mm$

TABLE 4 CONSTRAINTS OF EXAMPLE OPTIMIZATION.

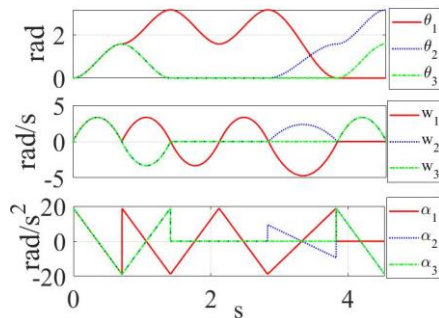| Joints max. cycle time $(t_{max.cycle})$	$1\ s$
Safety factor for motor $(0 < M_{sf} <1)$	0,9
Maximum payload (m_{max})	$1000\ g$
Sudden stop max. deceleration (af_{sudden})	2
Max. Harmonic Drive permissible twist $(\theta_{HD}$ 'arc-min')	$10\ arcmin$
Max. tip point error during motion $(err_{dynamic})$	$1\ mm$
Max. permissible static tip point error (err_{static})	$0,5\ mm$

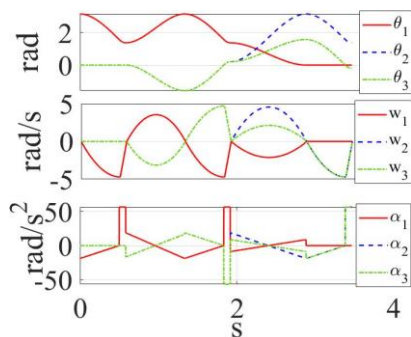Figure 8.   Nominal trajectory (cubic velocity profile).

Figure 9.   Sudden stop trajectory (trapezoidal velocity profile).

Figures 10 and 11 show the iterations of link thicknesses and, total weights of the robot during the optimization process respectively. In the optimization cycle, the drive-trains are determined first according to the desired robot performance via rigid body dynamic simulation. Then, the structure thicknesses were determined to overcome the end point error via flexible body dynamic simulation. However, after increasing the thicknesses of the structures, the dynamic performance decreases, and drive-trains become insufficient. Then, the drive-trains are changed with a bigger one and returned to the beginning of the optimization cycle. While returning, the thicknesses of the structures are reset and start with minimum thicknesses again. That is why there are sudden drops in Figure 10 and 11. Then, Figure 12 shows the necessary torques and motor capacity curves in nominal operations for final optimum design. As seen in Figure 12, necessary torques and motor capacity rate is maximum 0,9 which is the safety factor of the motor M_{sf} .
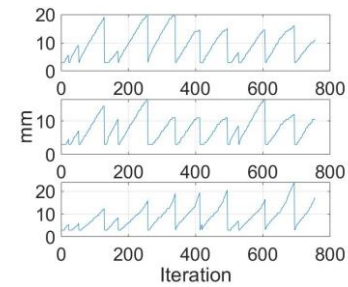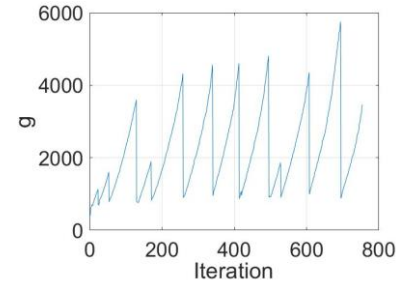

Figure 10. Link thickness iterations.

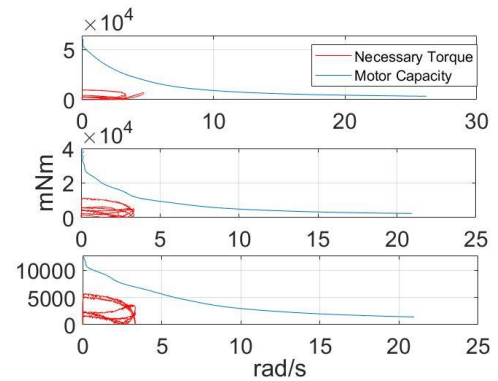Figure 11. Total robot weight iterations.

Figure 12. Necessary torques vs. motor capacity in nominal operation.

Figure 13 is obtained after a sudden stop dynamic simulation. It shows the comparison of the necessary torques in a sudden stop situation and Harmonic Drive momentary peak torque limit T_M for final optimum design. As shown in Figure 13, the selected Harmonic Drive gearboxes are durable enough for sudden stop deceleration. Then Figure 14 shows the tip point dynamic error graphic for the final optimum design. The errors are lower than the related constraint which is the maximum permissible tip point error during motion "$err_{dynamic} = 1\ mm$".
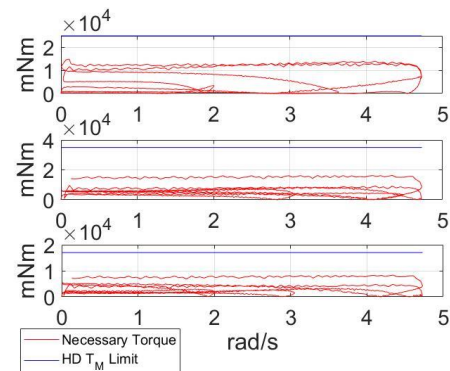
Figure 13. Necessary torques vs. Harmonic Drive T_M torque limit in sudden stop operation.

Then, Figure 15 and Table 5 show the final optimum robot manipulator view and the general results of optimum conceptual design respectively.
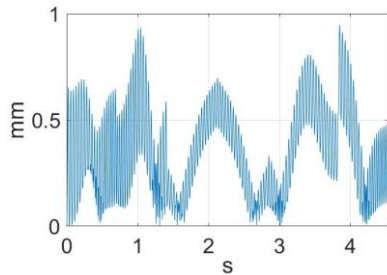

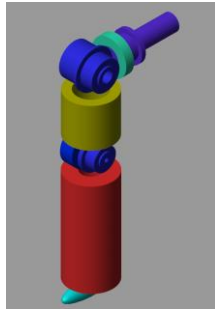Figure 14. Tip point error during motion for final optimum design.

Figure 15. Optimum Robot View.

TABLE 5 GENERAL RESULTS OF EXAMPLE OPTIMIZATION.

Maximum dynamic tip point error	$0,9477\ mm$
Maximum static tip point error	$0,1532mm$
Motor 1	EC-4POLE 22 90 W
Harmonic Drive gearbox 1	HFUC-2A-11-100
Link 1 thickness	$11\ mm$
Link 1 inner diameter	$24,7\ mm$
Link 1 outer diameter	$46,7\ mm$
Motor 2	EC45-50 W
Harmonic Drive gearbox 2	CPL-2A-14-80
Link 2 thickness	$10,5\ mm$
Link 2 inner diameter	$37\ mm$
Link 2 outer diameter	$58\ mm$
Motor 3	EC45-30 W
Harmonic Drive gearbox 3	HFUC-2A-11-50
Link 3 thickness	$17\ mm$
Link 3 inner diameter	$24,7\ mm$
Link 3 outer diameter	$58,7\ mm$
Total weight of robot	$3458\ g$
Number of iterations	755
Optimization duration	$166317\ s$

V. CONCLUSION

In this study, a new evolving conceptual design algorithm for a dynamic system is described and illustrated via a 3 DOF robot manipulator. This type of evolving conceptual design algorithm can be adapted to many kinds of dynamic systems to speed up the iteration process of design. Especially in robot design, the more powerful drive-trains not only increase the performance of the robot but also increase the total robot weight and deflections in the bodies. Then to overcome the deflection problem, the structure thicknesses are increased, hence the total weight increases again. This causes complexity in the design process and creates many iterations. Hence, structure and drive train concurrent optimization is necessary for some dynamic systems to increase efficiency and decrease deflections. The

optimization also decreases energy consumption. Integrated optimization both provides an optimum design and decreases the amount of time for the design. Especially, if the repeated designs are needed for different sizes of a similar dynamic system, an integrated design optimization that depends on design parameters and constraints becomes very helpful for the designer. It can also automatically design different sizes of the same system rapidly while ensuring the optimum design.

REFERENCES

[1] Kivelä, T., Mattila, J. And Puura, J.: A generic method to optimize a redundant serial robotic manipulator's structure, Automation in Construction 81, 172-179, http://dx.doi.org/10.1016/j.autcon.2017.06.006, 2017.

[2] Zhou, L., Bai, S. and Hansen, M. R.: Design optimization on the drive train of a light-weight robotic arm, Mechatronics 21, 560-569, https://doi.org/10.1016/j.mechatronics.2011.02.004, 2011a.

[3] Zhou, L., Bai, S. and Hansen, M. R.: Integrated dimensional and drive-train design optimization of a light-weight anthropomorphic arm, Robotics and Autonomous Systems 60, 113-122, https://doi.org/10.1016/j.robot.2011.09.004, 2012.

[4] Yin, H., Huang, S., He, M. and Li, J.: An overall structure optimization for a light-weight robotic arm, IEEE 11th Conference on Industrial Electronics and Applications, https://doi.org/10.1109/ICIEA.2016.7603872, 2016.

[5] Zhou, L., Bai, S. and Hansen, M. R.: Integrated Design Optimization of a 5-DOF Assistive Light-weight Anthropomorphic Arm, The 15th International Conference on Advanced Robotics, 978-1-4577-1159-6/11, https://doi.org/10.5281/zenodo.4661758, 2011b.

[6] Zhou, L. and Bai, S.: A New Approach to Design of a Lightweight Anthropomorphic Arm for Service Applications, Journal of Mechanisms and Robotics, https://doi.org/10.1115/1.4028292, Vol. 7 / 031001-1, 2015.

[7] Hwang, S., Kim, H., Choi, Y., Shin, K. and Han, C.: Design Optimization Method for 7 DOF Robot Manipulator Using Performance Indices, International Journal of Precision Engineering and Manufacturing, Vol. 18, No. 3, pp. 293-299, https://doi.org/10.1007/s12541-017-0037-0, 2017.

[8] Pettersson, M. and Ölvander, J.: Drive Train Optimization for Industrial Robots, IEEE Transactions on Robotics, Vol. 25, No. 6, pp. 1419-1424, https://doi.org/10.5281/zenodo.4661761, 2009.

[9] Ge, L. Z., Chen, J., Li, R. and Liang, P.: Optimization design of drive system for industrial robots based on dynamic performance, Industrial Robot.The International Journal of Robotics Research and Application, 44/6, 765-775, https://doi.org/10.1108/IR-10-2016-0251, 2017.

[10] Wang, X., Zhang, D., Zhao, C., Zhang, P., Zhang, Y. and Cai, Y.: Optimal design of lightweight serial robots by integrating topology optimization and parametric system optimization, Mechanism and Machine Theory 132, 48-65, https://doi.org/10.1016/j.mechmachtheory.2018.10.015 ,2019.

[11] Chen, J., Chen, Q. and Yang, H.: Additive manufacturing of a continuum topology-optimized palletizing manipulator arm, Mech. Sci., 12, 289–304, https://doi.org/10.5194/ms-12-289-2021, 2021.

[12] Ceccarelli, M. And Lanni, C.: A multi-objective optimum design of general 3R manipulators for prescribed workspace limits, Mechanism and Machine Theory 39, 119-132, https://doi.org/10.1016/S0094-114X(03)00109-5, 2004.

[13] Kucuk, S. and Bingul, Z.: Comparative study of performance indices for fundamental robot manipulators, Robotics and Autonomous Systems 54, 567-573, https://doi.org/10.1016/j.robot.2006.04.002,2006.

[14] Liang, M., Wang, B. and Yan, T.: Dynamic optimization of robot arm based on flexible multi-body model, Journal of Mechanical Science and Technology 31 (8), 3747~3754, https://doi.org/10.1007/s12206-017-0717-9, 2017.

[15] Li, H., Yang, Z. and Huang, T.: Dynamics and elasto-dynamics optimization of a 2-DOF planar parallel pick-and-place robot with flexible links, Structural and Multidisciplinary Optimization, 38:195–204, https://doi.org/10.1007/s00158-008-0276-x, 2008.

[16] Tromme, E., Brüls, O., Alt, J. E., Bruyneel, M., Virlez, G. and Duysinx, P.: Discussion on the optimization problem formulation of flexible components in multibody systems, Structural and Multidisciplinary Optimization, 48:1189–1206, https://doi.org/10.1007/s00158-013-0952-3, 2013.